Two-color light-emitting diodes with polarization-sensitive high extraction efficiency based on graphene

H Sattarian[1,†], S Shojaei[2], and E Darabi[1]

[1] *Plasma Physics Research Center, Science and Research Branch, Islamic Azad University, Tehran, Iran*
[2] *Photonics Department, Research Institute for Applied Physics & Astronomy, University of Tabriz, Tabriz, Iran*

(Received 18 August 2015; revised manuscript received 11 January 2016; published online 31 March 2016)

In the present study, graphene photonic crystals are employed to enhance the light extraction efficiency (LEE) of two-color, red and blue, light-emitting diode (LED). The transmission characteristics of one-dimensional (1D) Fibonacci graphene photonic crystal LED (FGPC-LED) are investigated by using the transfer matrix method and the scaling study is presented. We analyzed the influence of period, thickness, and permittivity in the structure to enhance the LEE. The transmission spectrum of 1D FGPC has been optimized in detail. In addition, the effects of the angle of incidence and the state of polarization are investigated. As the main result, we found the optimum values of relevant parameters to enhance the extraction of red and blue light from an LED as well as provide perfect omnidirectional and high peak transmission filters for the TE and TM modes.

Keywords: photonic crystal, blue light emitting diode, graphene, transfer matrix method

PACS: 85.60.Jb, 78.67.Wj, 42.70.Qs, 78.20.Ci **DOI:** 10.1088/1674-1056/25/5/058504

1. Introduction

Light-emitting diodes (LEDs) are small new-type low power, long lifetime, and convenient light sources that are used in backlight lighting of liquid crystal displays, automotive lighting, sign illuminations, and vehicle and traffic signals. For these and other advanced applications, LEDs with higher light output at lower power consumption are needed.[1] A source of white light needs LEDs that deliver red, green, and blue light. The first red LED was created in the 1950s and researchers then managed to create devices emitting light at shorter wavelengths, reaching green by the 1960s. However, researchers struggled to create blue light. The Nobel Prize in Physics 2014 was awarded jointly to Isamu Akasaki, Hiroshi Amano, and Shuji Nakamura "for the invention of efficient blue LEDs which has enabled bright and energy-saving white light sources".[2,3]

However, there is a problem in LED technology development denoting that the refractive index between air and the materials is large, resulting in the light produced by the active area having total internal reflection at the interface of materials with different refractive indexes, and not being extracted. Then the efficiency of these devices is limited due to the total internal reflection in the active region (e.g., semiconductor) interface and the outer medium. The critical angle of the total internal reflection is low (e.g., 18.4° for GaAs and 23° for GaN), so only a small fraction of light generated in the active region of the LED can escape into the outer environment. The light extraction efficiency (LEE) at the active region/air single interface is about $\sim 1/4n^2$.[4] Therefore, the external quantum efficiency of LEDs is poor even when the internal quantum efficiency is close to unity.

To avoid the above structural problem of LEDs and to extract more light from them, researchers have suggested several approaches, such as changing the LED chip shape,[5] nanohybrid structures,[6–8] micro-rods,[9] developed electron blocking layer structure,[10] photon recycling,[11] coupling to surface plasmonic modes,[12] roughening the surface[13,14] and metallic photonic crystal embedding in LED.[15] These approaches, however, do not alter directly the spontaneous emission properties of the devices. While, roughened surface, is an inexpensive to increase the light extraction efficiency, its morphology is irregular and uncontrolled. Recently, an approach using photonic crystals (PCs) was adopted and the LEE was enhanced dramatically. In this method, a two-dimensional (2D) PC is prepared in an LED surface in order to improve the LEE of LED surface using different periods of PC structures patterned in the surface.[16] The aim of this method is to avoid total internal reflection and to prevent lateral propagation of the light-waveguide effect and to enhance light extraction efficiency. The existence of a photonic band gap in a PC at the light emission wavelengths of LED modifies the guiding properties and reduces the waves propagating in lateral directions relative to the LED axis.[17] The enhancement of LEE in PC-LED occurs through a combination of spontaneous emission enhancement from a photonic crystal effect and Bragg scattering, which reduces parasitic absorption.[18]

Graphene, as a kind of gapless two-dimensional semiconductor, has attracted significant attention in recent years owing to its abundant potential application in nanoelectronic devices and optoelectronic devices. Due to the unique and

†Corresponding author. E-mail: h.sattarian@srbiau.ac.ir; hsattarian@yahoo.com

© 2016 Chinese Physical Society and IOP Publishing Ltd

extraordinary properties including high mobility of carriers, flexibility, robustness, environmental stability,[19,22] electronic energy spectrum without a gap between the conduction and valence bands, and frequency independent absorption of electromagnetic radiation, graphene has been the object of many recent experimental and theoretical studies in photonics.[23] This property makes graphene a suitable option for optoelectronic devices such as transparent electrodes, designing photonic devices, and optical display materials.[24,25] Recently, it has been shown that graphene can be used in tunable terahertz devices.[26,27] Improvement of the sensitivity of localized surface plasmon resonance (SPR) sensors by graphene was also reported.[28] One-dimensional graphene-based photonic crystals (1D-GPC), in which the graphene sheets are embedded between adjacent layers as a new type of transmission filter, attract considerable interest.[29]

Considering the benefits of using PCs as well as graphene, the present study attempts to explore how to enhance the LEE by considering the photonic band structure of one-dimensional Fibonacci quasi-periodic graphene photonic crystal (1D-FGPC). To reach this goal, we adopt the transfer matrix method to study the propagation of light through 1D-FGPC by using the optical conductivity of graphene.[30] Then, we theoretically introduce the optimized 1D-FGPC hybrid structure to design the high extracted red and blue LEDs.

2. Model and theoretical framework

According to the definition of light extraction efficiency $\eta_{\rm extr}$ of light emission from an LED, we have

$$\eta_{\rm extr}=\frac{N_{\rm emit}^{\rm free}}{N_{\rm emit}}, \tag{1}$$

where $N_{\rm emit}^{\rm free}$ is the number of photons emitted into free space per second and $N_{\rm emit}$ is the total number of photons emitted from the active layer per second. The external quantum efficiency is given as a product of the injection efficiency $\eta_{\rm inj}$ (the ratio of the number of electrons injected into the active region to the number of electrons injected into the device), the light extraction efficiency, and the internal quantum efficiency $\eta_{\rm int}$ (that is known to strongly depend on the injected carrier density). Since the internal quantum efficiency is the ratio of the radiative recombination rate $K_{\rm rad}$ to the total recombination rate $K_{\rm rad}+K_{\rm non}$, the equation for $\eta_{\rm ext}$ could be rewritten as

$$\begin{aligned}\eta_{\rm ext} &= \eta_{\rm extr}\eta_{\rm inj}\eta_{\rm int}\\ &= \eta_{\rm extr}\eta_{\rm inj}\frac{K_{\rm rad}}{K_{\rm rad}+K_{\rm non}}.\end{aligned} \tag{2}$$

From Eq. (2), we can find that there are different ways to increase the light output such as decreasing $K_{\rm non}$, increasing $K_{\rm rad}$, and increasing $\eta_{\rm extr}$.

We will find that the optimization of the transmission spectrum of 1D-FGPC enhances the LEE of LED.

In this work, one-dimensional 3rd-order Fibonacci quasi-periodic graphene photonic crystal is used to design the two-color transmission filters. The 1D-FGPC model is shown in Fig. 1. Here, A and B present two isotropic dielectric materials with the permittivity of $\varepsilon_{\rm A}$ and $\varepsilon_{\rm B}$ and thicknesses of $d_{\rm A}$ and $d_{\rm B}$, respectively. We assume that the layers are non-magnetic and their permeability is $\mu_{\rm A}=\mu_{\rm B}=1$. The structure in each dielectric cell follows the Fibonacci sequence, S_j, by a recurrent relation $S_{j+1}=\{S_j,S_{j-1}\}$ with $S_0=\{\rm B\}$, $S_1=\{\rm A\}$, and j being the generation number of the Fibonacci unit cell, the first few sequences are $S_2=\{\rm AB\}$, $S_3=\{\rm ABA\}$, $S_4=\{\rm ABAAB\}$, and so on. In this structure, the graphene monolayers are embedded between adjacent dielectric layers. The optical conductivity of a graphene sheet for typical frequency ω, at temperature T, is chosen as $\sigma_{\rm g}(\omega)=\sigma_{\rm g}^{\rm intra}(\omega)+\sigma_{\rm g}^{\rm inter}(\omega)$[31,32] which is based on the Kubo formula[33,34] as

$$\begin{aligned}&\sigma(\omega,\mu_{\rm c},\Gamma,T)\\ &=\frac{{\rm j}e^2(\omega-{\rm j}\Gamma)}{\pi\hbar^2}\left[\frac{1}{(\omega-{\rm j}\Gamma)^2}\int_0^\infty\left(\frac{\partial f_{\rm d}(\varepsilon)}{\partial\varepsilon}-\frac{\partial f_{\rm d}(-\varepsilon)}{\partial\varepsilon}\right)\varepsilon\,{\rm d}\varepsilon\right.\\ &\left.-\int_0^\infty\frac{f_{\rm d}(-\varepsilon)-f_{\rm d}(\varepsilon)}{(\omega-{\rm j}\Gamma)^2-4(\varepsilon/\hbar)^2}\,{\rm d}\varepsilon\right],\end{aligned} \tag{3}$$

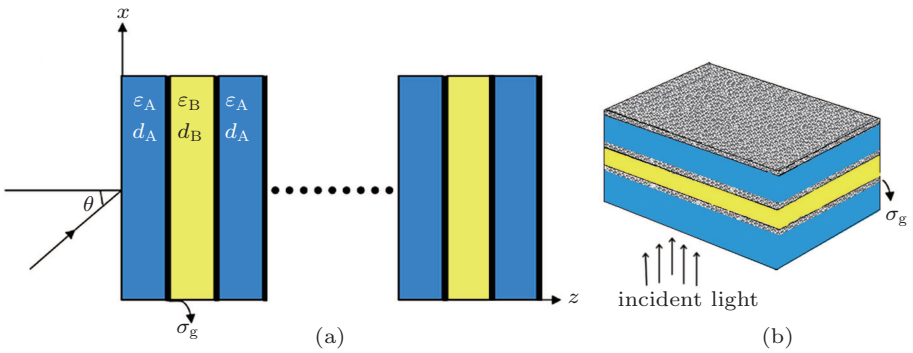


Fig. 1. (color online) (a) Structure of the 3rd-order 1D-FGPC. (b) Schematic diagram of unit cell for 1D-FGPC. The graphene monolayers are embedded between dielectric layers.

where e is the charge of an electron, $\hbar = h/(2\pi)$ is the reduced Planck's constant, $f_{\rm d}(\varepsilon) = (\mathrm{e}^{(\varepsilon-\mu_{\rm c})}+1)^{-1}$ is the Fermi–Dirac distribution, $k_{\rm B}$ is the Boltzmann constant, ε is the energy, $\mu_{\rm c}$ is the chemical potential determined by the electron concentration which can be controlled by gating, and Γ is the phenomenological scattering rate, which is assumed to be independent of energy ε. The first term in Eq. (3) is due to intraband contributions and the second term in Eq. (3) is due to interband contributions, and can be evaluated in the following closed forms:[31,35]

$$\sigma_{\rm g}^{\rm intra}(\omega) = -\mathrm{j}\frac{e^2 k_{\rm B} T}{\pi\hbar^2(\omega-\mathrm{j}\Gamma)} \times \left[\frac{\mu_{\rm c}}{k_{\rm B}T} + 2\ln(\mathrm{e}^{-\mu_{\rm c}/k_{\rm B}T}+1)\right], \quad (4)$$

$$\sigma_{\rm g}^{\rm inter}(\omega) = \frac{-\mathrm{j}e^2}{4\pi\hbar}\ln\left(\frac{2|\mu_{\rm c}|-(\omega-\mathrm{j}\Gamma)\hbar}{2|\mu_{\rm c}|+(\omega-\mathrm{j}\Gamma)\hbar}\right). \quad (5)$$

With the propagation of light across an interface formed by a graphene layer which separates two dielectrics, there will be surface current in the graphene layer. The surface current density J of the graphene layer can be obtained from Ohm's law, namely, $J_x = \sigma E_x$ for TM waves and $J_y = \sigma E_y$ for TE waves. According to the expressions of electric and magnetic fields, the boundary conditions and the propagation matrix of light in a homogenous medium, we obtain the transfer matrix $M_j(d_j,\omega)\,(j = \mathrm{A},\mathrm{B})$ of a dielectric layer and a graphene sheet for TE and TM waves as[29]

$$M_j(d_j,\omega) = \begin{pmatrix} \cos(k_{zj}d_j) & (\mathrm{i}/q_j)\sin(k_{zj}d_j) \\ \sigma_{\rm g}\cos(k_{zj}d_j)+\mathrm{i}q_j\sin(k_{zj}d_j) & (\mathrm{i}\sigma_{\rm g}/q_j)\sin(k_{zj}d_j)+\cos(k_{zj}d_j) \end{pmatrix}, \quad (6)$$

$$M_j(d_j,\omega) = \begin{pmatrix} \cos(k_{zj}d_j)-(\mathrm{i}\sigma_{\rm g}/q_j)\sin(k_{zj}d_j) & \mathrm{i}q_j\sin(k_{zj}d_j)-\sigma_{\rm g}\cos(k_{zj}d_j) \\ \mathrm{i}\sigma_{\rm g}/q_j\sin(k_{zj}d_j) & \cos(k_{zj}d_j) \end{pmatrix}. \quad (7)$$

Here, $q_j = (-k_{zj}/\omega\mu_0\mu_j)$ for TE waves and $q_j = (+k_{zj}/\omega\varepsilon_0\varepsilon_j)$ for TM waves and q_0 and $q_{\rm t}$ are defined as the corresponding q parameters of the input and exit media (corresponding to medium that light travels in it before and after 1D FGPC) which their permittivities are chosen as 1.6 and 1, respectively. Our calculations show that for TE waves, changing the value of permittivity of the active medium does not remarkably alter the value and position of the peaks (corresponding to blue and red light) of the transmission coefficient, in contrast to the case of TM waves. Thus, the final transfer matrix $T_2(=M_{\rm A}M_{\rm B})$, $T_3(=M_{\rm A}M_{\rm B}M_{\rm A})$, and $T_4(=M_{\rm A}M_{\rm B}M_{\rm A}M_{\rm A}M_{\rm B})$ refer to S_2, S_3, and S_4 structures, respectively. Then, from the entire transfer matrix one can obtain the transitivity T, reflectivity R, and absorptivity A of the structure as

$$T = \left|\frac{2q_0}{(q_{\rm t}T_{11}+q_0T_{22})-(T_{21}+q_0q_{\rm t}T_{12})}\right|^2, \quad (8)$$

$$R = \left|\frac{(q_{\rm t}T_{11}-q_0T_{22})-(T_{21}-q_0q_{\rm t}T_{12})}{(q_{\rm t}T_{11}+q_0T_{22})-(T_{21}+q_0q_{\rm t}T_{12})}\right|^2, \quad (9)$$

$$A = 1-R-T. \quad (10)$$

Here, T_{11}, T_{12}, T_{21}, and T_{22} are the elements of the total transfer matrix.

3. Results and discussion

In this section, we choose the optimum values of optical and geometrical parameters ($d_{\rm A}$, $d_{\rm B}$, $\varepsilon_{\rm A}$, $\varepsilon_{\rm B}$) of the system for red and blue light frequencies (about 440 THz and 630 THz, respectively). To find optimized parameters, in Fig. 2, the effects of $d_{\rm A}$, $d_{\rm B}$, $\varepsilon_{\rm A}$, $\varepsilon_{\rm B}$, thickness and permittivity of layers A and B, on transmission spectrum are presented for normal incidence (when the angle between the wave vector of the incidence light and multilayer extension is 0°). From Figs. 2(a) and 2(b), the range of values in which maximum values of transmission occurred is clear. We choose: $d_{\rm A} = 96$ nm, $d_{\rm B} = 94$ nm, $\varepsilon_{\rm A} = 14.6$, $\varepsilon_{\rm B} = 5.9$, $\mu_{\rm C} = 0.2$ eV, $T = 300$ K, and $\Gamma = 0$. Calculations show that the changing of $\mu_{\rm C}$ from 0 to 1 eV does not have remarkable effect on transmission spectrum, but for higher values, i.e., values between 1 eV to 1.5 eV, the peaks of transmission spectrum reach 1 without any shift in frequency. For $\mu_{\rm C}$ larger than 1.5 eV, the peak positions and their values are not changed.

Our calculations show that for higher-order Fibonacci quasi-periodic 1D-GPC (4th, ...) transmission spectrum will be decreased. Therefore, we focused on the 3rd-order Fibonacci quasi-periodic graphene photonic crystal of 1 period. Figure 3 demonstrates the transmission spectrum of 1D-FGPC (T_3) structure with and without graphene sheets as a function of the light frequency. The optical transmission of the 1D-FGPC with graphene is about 97.35 percent (solid red curve). In contrast, in the structure without the graphene, transmission is about 100 percent (dotted blue curve). The transmission peaks correspond to the chosen optimum values of the parameters, which can be used in designing two-color transmission filters or in enhancing the extraction of red–blue light from an LED.

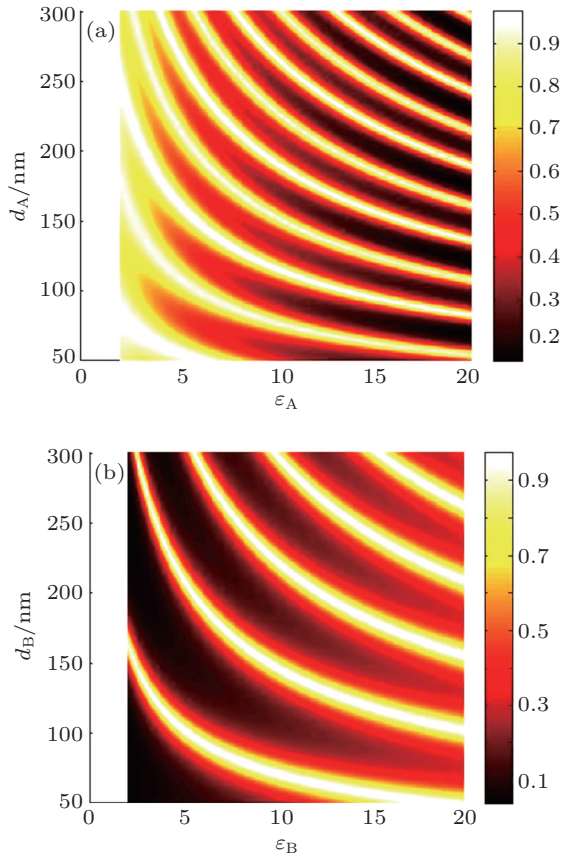


Fig. 2. (color online) Contour plots of the transmission spectrum of the 1D-FGPC (T_3) structure as a function of the permittivities and thicknesses in the case of $\sigma_g \neq 0$ and blue light frequency for the dielectric material A (a) and the dielectric material B (b). The waves are normal incidence to the interfaces and temperature and chemical potential are chosen as $T = 300$ K and $\mu_C = 0.2$ eV.

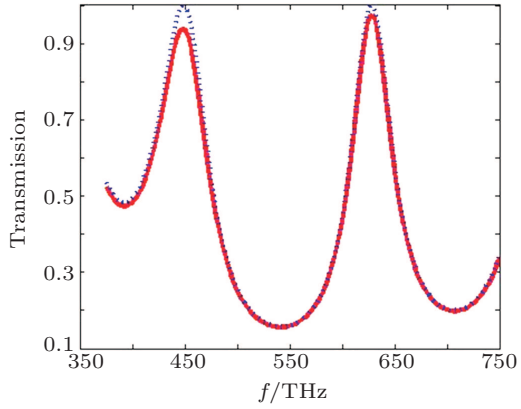


Fig. 3. (color online) The transmission spectrum of 1D-FGPC (T_3) structure as a function of the light frequency in the cases of (a) $\sigma_g \neq 0$ (solid red curve) and (b) $\sigma_g = 0$ (dotted blue curve) for the normal incidence of the waves. Temperature and chemical potential are chosen as $T = 300$ K and $\mu_C = 0.2$ eV.

For oblique incidence ($\theta \neq 0°$), transmission spectrum of 1D FGPC (T_3) structure is calculated with graphene sheets as a function of the light frequency for different incident angles plotted in Figs. 4 and 5. It is clear that for $\theta = 0°$, the locations of the peaks in the TM and TE modes completely overlap. The transmission peaks move toward larger frequencies by increasing incident angle θ both for TE and TM modes. For the TE mode, when θ increases, the transmission peak of light becomes narrower (peaks occurred at mono-color frequency) and the value of transmission is reduced slightly. In the TM mode, as the incident angle increases, the transmission is enhanced but the peaks become wider so that, for a wide range of frequencies from about 530 THz to 650 THz, transmission approximates to 1. The reason is that in the TE polarization the surface current is inversely proportional to k_z (the z component of the wave-vector),[30] the gaps broaden with the increase of incident angle. This result is in total consistency with the findings of Zhang *et al.*[35] In contrast, for TM polarization, the surface current is proportional to k_z, so the gaps become narrower, meanwhile they shift to high frequency.

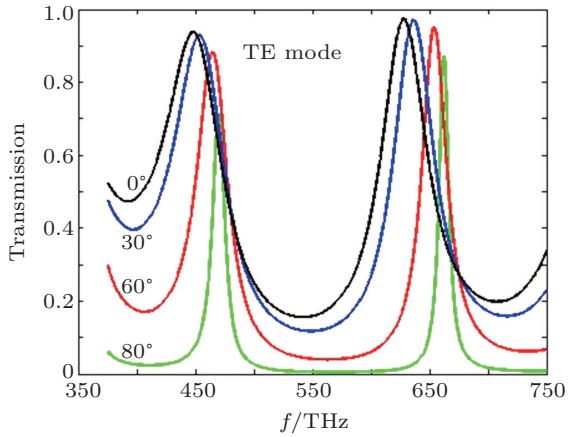


Fig. 4. (color online) Transmission spectrum of 1DGPC (T_3) structure in the case of $\sigma_g \neq 0$ as a function of the light frequency for different incident angles in the TE mode: $\theta = 0°$ (black curve), $\theta = 30°$ (blue curve), $\theta = 60°$ (red curve), and $\theta = 80°$(green curve).

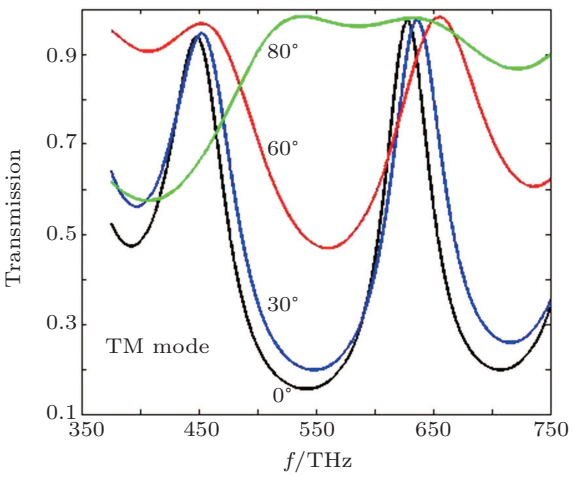


Fig. 5. (color online) Transmission spectrum of 1DGPC (T_3) structure in the case of $\sigma_g \neq 0$ as a function of the light frequency for different incident angles in the TM mode: $\theta = 0°$ (black curve), $\theta = 30°$ (blue curve), $\theta = 60°$ (red curve), and $\theta = 80°$ (green curve).

The findings demonstrate that our model structure is suitable for enhancing the mono-color light extraction efficiency of TE mode in (red or blue) LEDs. In addition, in the case of TM mode, it is useful to enhance the LEE in a wide range of visual frequencies.

To find out more, we consider the dependence of photonic band gap (PBG) on the incidence angle with graphene as a function of the light frequency and the incident angle. The results are displayed in Fig. 6. The gaps are represented by the dark areas while the bright areas show the allowed bands. It is clear that the PBG is sensitive to polarization and depends strongly on the incident angle which is the characteristic of the conventional Bragg gap. From this figure, it can be deduced that for TE mode, the transmission of red and blue light is enhanced in the whole range of incident angles (0 to almost 90°); while, for TM mode, for incident angles larger than almost 70°, transmission is enhanced for all visible frequencies.

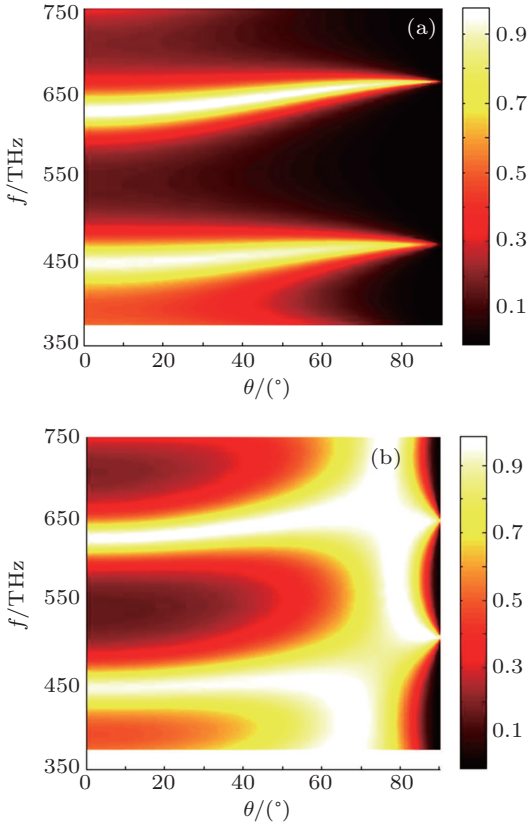


Fig. 6. (color online) Contour plots of the transmission spectrum of the 1D-FGPC (T_3) structure as a function of the light frequency and the incident angle with graphene sheets for TE waves (a) and TM waves (b).

4. Conclusion

In conclusion, we employed the proposed 1D-FGPC hybrid structure and optimized relevant parameters for the red–blue LEDs with the transfer matrix method. An optimized structure in terms of thickness, number of periods, layers, refractive indices, and permittivity of materials has been obtained. The 1D-FGPC filters with high transmission rates of 93.8 percent and 97.38 percent are located in the red and blue light frequencies (448.2 THz and 628.1 THz, respectively) for the normal incidence of the waves. The new graphene-photonic heterostructure provides perfect omnidirectional and high peak transmission filters for the TE and TM modes. This Fibonacci structure provides potentiality for fabricating red–blue two-color filters in the visible band and also for enhancing the extraction of red–blue light from an LED.

References

[1] Wierer J J, David A and Megens M M 2009 *Nat. Photon.* **3** 163
[2] Yasushi N 2014 *Nat. Photon.* **8** 884
[3] Weisbuch C, Piccardo M, Martinelli L, Iveland J, Peretti J and Speck J S 2015 *Phys. Status Solidi A* **212** 899
[4] Smith J V 1982 *Geometrical and Structural Crystallography* (New York: Smith and Wyllie Intermediate Geology Series)
[5] Fujii T, Gao Y, Sharma R, Hu E L, DenBaars S P and Nakamura S 2004 *Appl. Phys. Lett.* **84** 855
[6] Son T, Jung K Y and Park J 2013 *Current Appl. Phys.* **13** 1042
[7] Xia Z L, Guo Y Z, Bo S, Chao Z S, Bo A P, Chao Y, Lei L, Xi W J and Min L J 2015 *Chin. Phys. B* **24** 068506
[8] Carr W N and Pittman G E 1963 *Appl. Phys. Lett.* **3** 173
[9] Yang D C, Wang D S, Zhang K X, *et al.* 2014 *Chin. Phys. Lett.* **31** 027101
[10] Wang T H, Xu J L and Wang X D 2013 *Physica E* **47** 51
[11] Schnitzer I, Yablonovitch E, Caneau C and Gmitter T J 1993 *Appl. Phys. Lett.* **62** 131
[12] Chen Z X, Wan W, Zhang B J, He Y J and Jin C J 2014 *Chin. Phys. B* **23** 128504
[13] Schnitzer I, Yablonovitch E, Caneau C, Gmitter T J and Scherer A 1993 *Appl. Phys. Lett.* **63** 2174
[14] Kim D W, Lee H Y, Yoo M C and Yeom G Y 2005 *Appl. Phys. Lett.* **86** 052108
[15] Chen J, Wang Q and Li H 2011 *Optik* **122** 1079
[16] Pudis D, Suslik L, Skriniarova J, Kovac J, Jr. J K, Kubicova I, Martincek I, Hascik S and Schaaf P 2013 *Appl. Surf. Sci.* **269** 161
[17] Andreani L C and Agio M 2002 *IEEE J. Quantum Electron.* **38** 891
[18] Chen L, Nurmikko A V and Krames M 2004 *Conferenc on Lasers and Electro-Optics* (San Francisco, California, United States)
[19] Bonaccorso F, Sun Z, Hasan T and Ferrari A C 2010 *Nat. Photon.* **4** 611
[20] Stauber T, Peres N M R and Geim A K 2008 *Phys. Rev. B* **78** 085432
[21] Soldano C, Mahmood A and Dujardin E 2010 *Carbon* **48** 2127
[22] Singh V, Joung D, Zhai L, Das S, Khondaker S I and Seal S 2011 *Prog. Mater. Sci.* **56** 1178
[23] Neto A H C, Guina F, Peres N M R, Novoselov K S and Geim A K 2009 *Rev. Moden. Phys.* **81** 109
[24] Wang X, Zhi L and Miilen K 2008 *Nano Lett.* **8** 323
[25] Liu J T, Liu N H, Li J, Li X J and Huang J H 2012 *Appl. Phys. Lett.* **101** 052104
[26] Zhang Y, Li T, Zeng B, Zhang H, Lv H, Huang X, Zhang W and Azad A K 2015 *Nanoscale* **7** 12682
[27] Zhang Y P, Li T T, Lv H H, Huang X Y, Zhang X, Xu S L and Zhang H Y 2015 *Chin. Phys. Lett.* **32** 068101
[28] Simsek E and Member S 2013 *IEEE Photon. Technol. Lett.* **25** 867
[29] Madani A and Roshan E S 2013 *Physica B* **431** 1
[30] Zhan T, Shi X, Dai Y, Liu X and Zi J 2013 *J. Phys.: Condens. Matter* **25** 215301
[31] Falkovsky L A and Pershoguba S S 2007 *Phys. Rev. B* **76** 153410
[32] Falkovsky L A 2008 *J. Phys.: Conf. Ser.* **129** 012004
[33] Hanson G W 2008 *J. Appl. Phys.* **103** 064302
[34] Gusynin V P, Sharapov S G and Carbotte J P 2007 *J. Phys.: Condens. Matter* **19** 026222
[35] Zhang Y, Wu Z, Cao Y and Zhang H 2015 *Opt. Commun.* **338** 168